

Pressure induced modification of electronic and magnetic properties of MnCrNbAl and MnCrTaAl

Brandon Schmidt,¹ Paul M. Shand,¹ Parashu Kharel,² Pavel V. Lukashev^{1, #}

¹*Department of Physics, University of Northern Iowa, Cedar Falls, IA 50614, USA*

²*Department of Chemistry, Biochemistry, and Physics, South Dakota State University, Brookings, SD 57007, USA*

Corresponding author: pavel.lukashev@uni.edu

Abstract

Spin-gapless semiconductor (SGS) is a new class of material that has been studied recently for potential applications in spintronics. This material behaves as an insulator for one spin channel, and as a gapless semiconductor for the opposite spin. In this work, we present results of a computational study of two quaternary Heusler alloys, MnCrNbAl and MnCrTaAl that have been recently reported to exhibit spin-gapless semiconducting electronic structure. In particular, using density functional calculations we analyze the effect of external pressure on electronic and magnetic properties of these compounds. It is shown that while these two alloys exhibit nearly SGS behavior at optimal lattice constants and at negative pressure (expansion), they are half-metals at equilibrium, and magnetic semiconductors at larger lattice constant. At the same time, reduction of the unit cell volume has a detrimental effect on electronic properties of these materials, by modifying the exchange splitting of their electronic structure and ultimately destroying their half-metallic / semiconducting behavior. Thus, our results indicate that both MnCrNbAl and MnCrTaAl may be attractive for practical device applications in spin-based electronics, but a potential **compression of the unit cell volume** (e.g. in thin-film applications) should be avoided.

I. Introduction

Generation of highly spin-polarized current is one of the main components for designing modern spintronic devices. As an example of practical implementation, the magnetization in magnetic random-access memories (MRAM) may be reversed by a spin-polarized current (spin-transfer torque (STT)) rather than by magnetic fields.¹ Materials that are typically used for such applications are Co-Fe ferromagnetic metals. They are used, for example, in magnetic tunnel junctions (MTJs) utilizing the effect of tunneling magnetoresistance (TMR). In these systems, the

electrical conductance depends on the orientation of magnetization in the ferromagnetic electrodes.² In principle, the ideal candidate for applications that require a highly spin-polarized current is a half-metal, a material that provides 100% spin-polarization by definition. Here, the spin-polarization P is defined as $P = \left| \frac{N_{\uparrow}(E_F) - N_{\downarrow}(E_F)}{N_{\uparrow}(E_F) + N_{\downarrow}(E_F)} \right|$, where $N_{\uparrow\downarrow}(E_F)$ is the spin-dependent density of states (DOS) at the Fermi level, E_F .³ The half-metallic compounds exhibit metallic conductivity for one spin-channel and insulating behavior for the opposite spin, resulting in 100% spin-polarization. Many systems have been reported to exhibit half-metallic behavior, of which Heusler alloys attracted particular attention, mostly because of their high Curie temperature.^{4,5,6,7,8,9,10}

In addition to half-metallic systems, a new class of materials, namely spin-gapless semiconductors (SGS) have attracted significant attention in recent years, mostly because of their potential applications in the emerging field of semiconductor spintronics. Spin-gapless semiconductor is a material with semiconducting band structure for one spin channel, and gapless band structure for the opposite spin. Thus, ideally SGS materials should provide semiconducting electron transport and the spin-polarization of the current close to 100%. The concept of spin-gapless semiconductivity was suggested by X. L. Wang in 2008.¹¹ In SGS materials, both electrons and holes can be fully spin polarized. The characteristic feature of a gapless semiconductor (the most famous example of which is graphene) is that no energy is needed to excite electrons from the valence band to the conduction band. Several systems have been reported to exhibit SGS behavior, for example oxides such as Co-doped PbPdO₂¹¹ and Heusler compounds such as Mn₂CoAl, CoCrFeAl, and FeCrTiAl.^{12,13,14,15,16} In principle, achieving robust SGS behavior in a given system may be challenging, since many factors, such as atomic vacancies and other lattice imperfections may have a detrimental impact on SGS character of a candidate material.¹⁷

In this work, we employ first principles calculations to study two quaternary Heusler alloys, MnCrNbAl and MnCrTaAl, that have been recently reported to exhibit SGS behavior.¹⁵ We show that while both materials indeed demonstrate SGS-resembling electronic structure in the ground state and under expansion of the unit cell volume, they are actually half-metals at equilibrium and magnetic semiconductors at larger lattice constants. At the same time, reduction of the unit cell volume below its equilibrium value destroys the half-metallic character of these alloys by modifying their exchange splitting, and ultimately making both **spin-up and spin-down** channels conducting.

II. Computational methods

The results reported in this work are obtained using density functional calculations, as implemented in the Vienna *ab initio* simulation package (VASP).¹⁸ We used the projector augmented-wave method (PAW)¹⁹ and generalized-gradient approximation (GGA) method proposed by Perdew, Burke, and Ernzerhof,²⁰ as well as the integration method by Methfessel and Paxton with a 5×10^{-2} eV width of smearing.²¹ The electronic and magnetic structure calculations are performed with the energy convergence criterion of 10^{-3} meV and with a k -mesh of $8 \times 8 \times 8$. We used the MedeA® software environment²² for visualizing the crystal structures (not included in the text). The reported calculations were performed using the Advanced Cyberinfrastructure Coordination Ecosystem: Services & Support (ACCESS) (formerly known as Extreme Science and Engineering Discovery Environment (XSEDE)) resources located at the Pittsburgh Supercomputing Center (PSC)²³, the resources of the Center for Functional Nanomaterials (CFN) at Brookhaven National Laboratory (BNL), as well as the high-performance computing facilities located at the University of Northern Iowa (UNI).

III. Results

MnCrNbAl and MnCrTaAl belong to a class of regular cubic Heusler alloys (space group F-43m). The Wyckoff positions of the atoms are as follows: Mn (0,0,0), Cr (1/2,1/2,1/2), Nb/Ta (3/4,3/4,3/4), Al (1/4,1/4,1/4). The calculated equilibrium lattice constants of MnCrNbAl and MnCrTaAl are 6.079 Å and 6.054 Å, correspondingly, in agreement with a recent report by Gao, Opahle, and Zhang.¹⁵ The magnetic alignment of both MnCrNbAl and MnCrTaAl is ferrimagnetic. Table 1 shows the calculated magnetic moments at the equilibrium lattice constants. As one can see from the table, the ferrimagnetic nature is due to the magnetic moments of Nb / Ta being anti-aligned with the magnetic moments of Mn and Cr (the magnetic moment of Al is negligible and is not shown in the table). A small difference between the sum of the individual magnetic moments and the total magnetic moment is due to the fact that the local magnetization and charge are calculated in atomic spheres that do not precisely fill the volume of the unit cell.¹²

Figure 1 shows calculated density of states at the equilibrium lattice constants of MnCrNbAl (a) and MnCrTaAl (b). Both compounds demonstrate nearly spin-gapless semiconducting electronic structure. In particular, for both alloys there is an energy gap at the **spin-**

up channel right above the Fermi level. At the same time, the **spin-down** DOS exhibits nearly gapless character around the Fermi level.

Magnetic moment	Mn (μ_B /atom)	Cr (μ_B /atom)	Nb/Ta (μ_B /atom)	Total (μ_B /f.u.)
MnCrNbAl	1.282	2.095	-0.446	2.993
MnCrTaAl	1.199	2.053	-0.340	2.983

Table 1. Calculated atom resolved and total magnetic moments of MnCrNbAl (second row) and MnCrTaAl (third row) at equilibrium lattice constants.

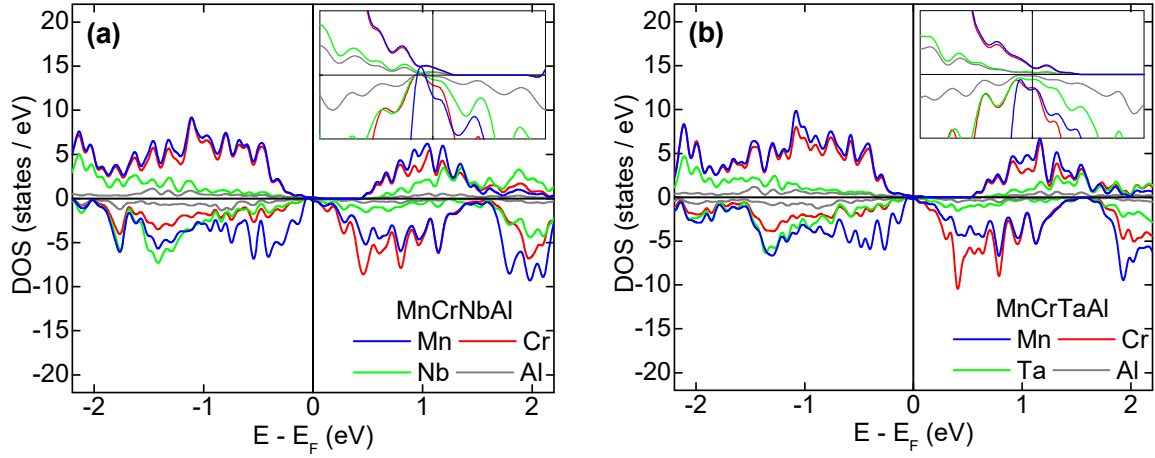


Figure 1. Calculated element-resolved density of states of MnCrNbAl (a) and MnCrTaAl (b) at the ground state lattice parameters. Positive DOS corresponds to **spin-up**, negative DOS corresponds to **spin-down** states. The atomic contributions are colored as follows: Mn – blue, Cr – red, Nb / Ta – green, Al – gray. Vertical line indicates position of the Fermi level. **The insets show the enlarged version of DOS around Fermi level.**

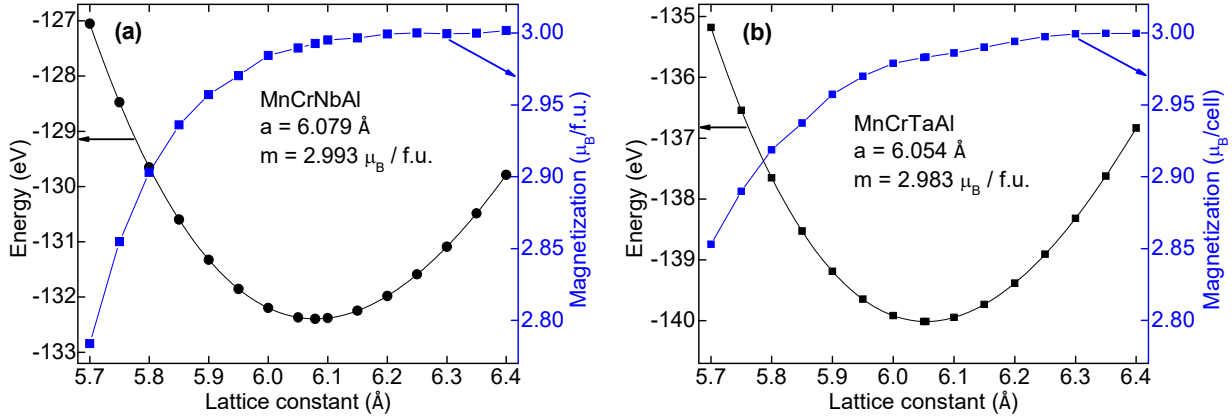


Figure 2. Calculated energy (black line and circles) and magnetization (blue line and squares) of MnCrNbAl (a) and MnCrTaAl (b) under hydrostatic pressure as a function of lattice constant.

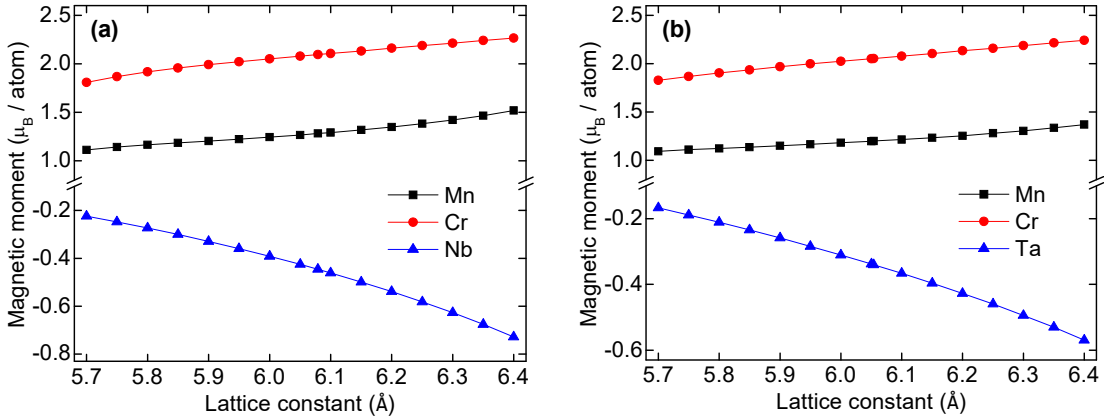


Figure 3. Calculated element-resolved magnetic moments of MnCrNbAl (a) and MnCrTaAl (b) under hydrostatic pressure as a function of lattice constant. Mn – black line and squares, Cr – red line and circles, Nb / Ta – blue line and triangles.

In practical device applications, such as in thin-film heterostructures, the materials are often exposed to a significant degree of mechanical strain. It is, therefore, important to know how the electronic and magnetic properties of the materials intended for such applications respond to external pressure. Figure 2 shows calculated energy (black line and circles) and magnetization (blue line and squares) of MnCrNbAl (a) and MnCrTaAl (b) under hydrostatic (uniform) pressure as a function of lattice constant. As one can see from the figure, the magnetization of both MnCrTaAl and (especially) MnCrNbAl reaches integer value of $3.00 \mu_B/\text{f.u.}$ at the lattice constants above equilibrium values. The integer magnetization value may serve as an indication of 100% spin-polarized electronic structure. Indeed, for 100% spin-polarized compounds, such as half-metals and spin-gapless semiconductors, the states in the valence band of one of the spin channels are fully occupied, thus making the number of these states an integer. As the total valence charge is an integer, such electronic structure results in an integer total magnetic moment per formula unit.²⁴

Figure 3 shows calculated element-resolved magnetic moments of MnCrNbAl (a) and MnCrTaAl (b) under uniform pressure as a function of lattice constant. As one can see from the figure, the increase of the unit cell volume results in increase (by absolute value) of the atomic magnetic moments. The total magnetic moment, however, is only moderately affected by the change in the lattice parameter because of the ferrimagnetic nature of these compounds, i.e. the increase of the magnetic moments of Mn and Cr is partially compensated by the increase of the anti-aligned magnetic moments of Nb / Ta.

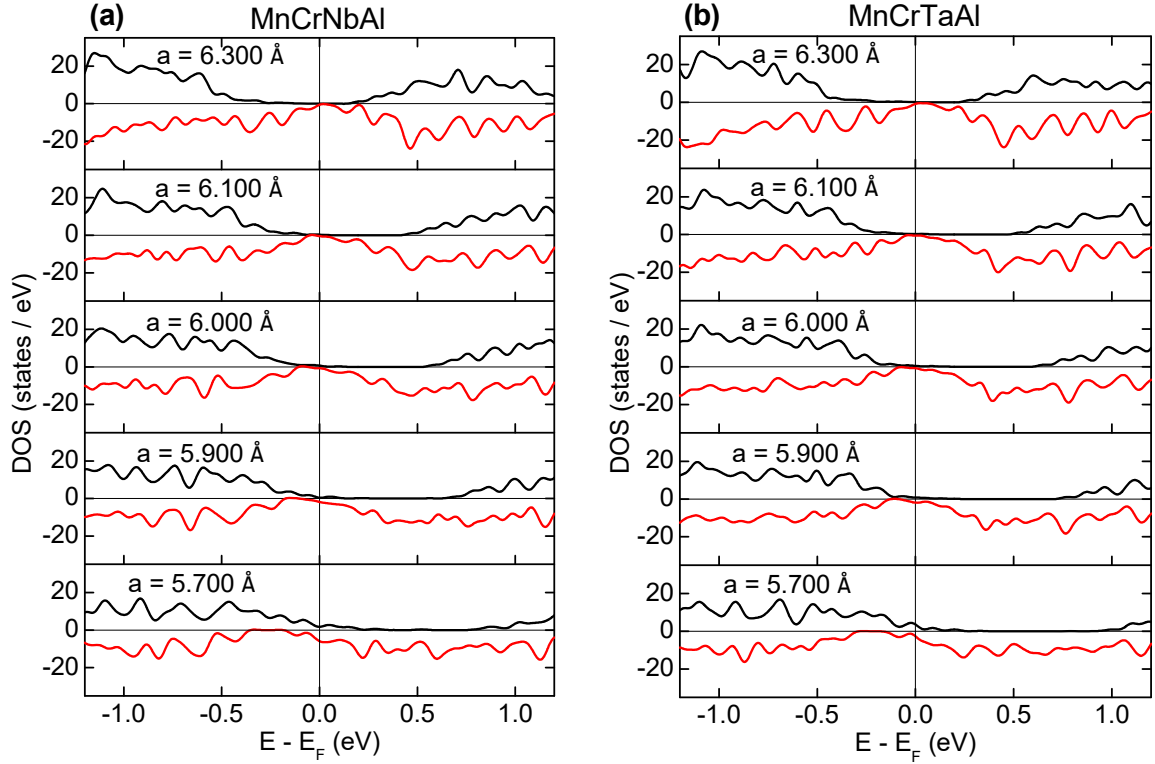


Figure 4. Calculated total density of states of MnCrNbAl (a) and MnCrTaAl (b) under hydrostatic pressure as a function of lattice constant. Positive DOS (black line) corresponds to **spin-up**, negative DOS (red line) corresponds to **spin-down** states. Lattice constants at which DOS is calculated are shown in the figure. Vertical line indicated position of the Fermi level.

Figure 4 shows calculated total density of states of MnCrNbAl (a) and MnCrTaAl (b) under uniform pressure as a function of lattice constant. As is evident from the figure, the reduction of the unit cell volume has a detrimental impact on SGS character of both MnCrNbAl and MnCrTaAl. A close inspection of the figure shows that the main effect of the pressure is in modifying the exchange splitting for both of these materials. More specifically, decrease of the lattice constant increases the population of the minority-spin states, while simultaneously decreasing the population of the **spin-up** states. As a result, both **spin-up** and **spin-down** spin channels of both MnCrNbAl and MnCrTaAl exhibit metallic behavior at smaller lattice constants. At the same time, the **spin-up** states are insulating at equilibrium and larger lattice parameters. As for the **spin-down** states, although their profile around Fermi energy somewhat resembles an SGS characteristics at equilibrium and larger lattice constants, a closer inspection actually reveals that there is a small energy gap for these states as well. This is illustrated in Figure 5 which shows the calculated band

structure of MnCrNbAl (the band structure of MnCrTaAl exhibits similar behavior and is not shown here).

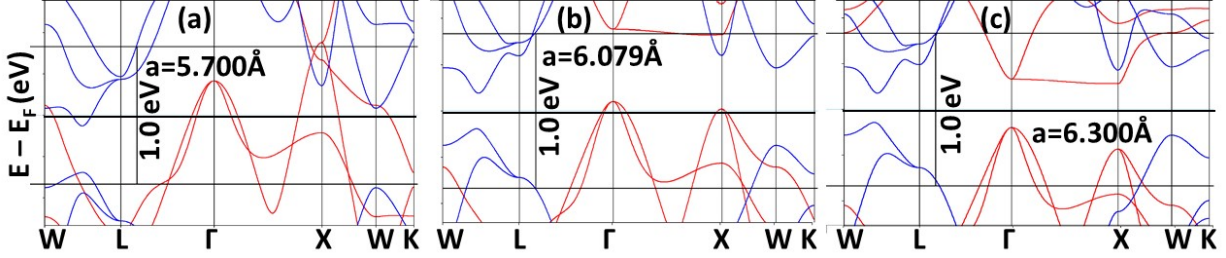


Figure 5. Calculated band structure of MnCrNbAl at the lattice constants of 5.700 Å (a), 6.079 Å (b), and 6.300 Å (c). Red line corresponds to spin-up states, blue line to spin-down states. An energy window of 1.00 eV is shown by two bold horizontal lines connected by a vertical line.

As one can see from Figure 5, at equilibrium lattice parameter MnCrNbAl is half-metallic, while at larger lattice parameters it has an electronic structure of a magnetic semiconductor (MnCrTaAl exhibits a similar behavior). The transition from half-metallic to semiconducting state is induced by a shift of the **spin-up** valence band maximum below Fermi level at the Γ point (see Fig. 5 (c)). At the same time, at the lattice constants smaller than equilibrium values, these compounds exhibit metallic behavior. Thus, these compounds may be appealing for practical spintronic applications at their equilibrium and larger lattice constants, but reduced unit cell volume may have a detrimental effect on their electronic structure.

IV. Conclusions

Here, we presented results of first principles study of two quaternary Heusler alloys, MnCrNbAl and MnCrTaAl that have been recently reported to exhibit spin-gapless semiconducting electronic structure. In particular, using density functional calculations we analyzed the effect of external pressure on electronic and magnetic properties of these compounds. We showed that these two alloys exhibit near SGS behavior at optimal lattice constants and at negative pressure (expansion). More specifically, at equilibrium these materials are half-metallic, while at larger lattice parameters they exhibit magnetic semiconducting properties. At the same time, reduction of the unit cell volume has a detrimental effect on electronic structure of these materials, ultimately destroying their half-metallic / semiconducting behavior. We hope that the

presented results may be interesting for researchers working on practical applications of materials intended for spin-based electronic devices.

Acknowledgments

This research is supported by the *National Science Foundation* (NSF) under Grant Numbers 2003828 and 2003856 via DMR and EPSCoR. This work used the Advanced Cyberinfrastructure Coordination Ecosystem: Services & Support (ACCESS) (formerly known as Extreme Science and Engineering Discovery Environment (XSEDE)), which is supported by National Science Foundation grant number ACI-1548562. This work used the XSEDE Regular Memory (Bridges 2) and Storage (Bridges Ocean) at the Pittsburgh Supercomputing Center (PSC) through allocation TG-DMR180059, and the resources of the Center for Functional Nanomaterials, which is a U.S. DOE Office of Science Facility, and the Scientific Data and Computing Center, a component of the Computational Science Initiative, at Brookhaven National Laboratory (BNL) under Contract No. DE-SC0012704.

Data Availability

The data that support the findings of this study are available from the corresponding author upon reasonable request.

References

- ¹ E. Tsymbal, *Nature Materials* **11**, 12–13 (2012).
- ² E. Tsymbal, O. Mryasov, and P. LeClair, *J. Phys.: Condens. Matter* **15** R109 (2003).
- ³ J. Velev, P. Dowben, E. Tsymbal, S. Jenkins, and A. Caruso, *Surf. Sci. Rep.* **63**, 400 (2008).
- ⁴ R. de Groot, F. Mueller, P. van Engen, and K. Buschow, *Phys. Rev. Lett.* **50**, 2024 (1983).
- ⁵ I. Galanakis, P. Dederichs, N. Papanikolaou, *Phys. Rev. B* **66**, 174429 (2002).
- ⁶ E. Şaşioğlu, L. Sandratskii, and P. Bruno, *Phys. Rev. B* **72**, 184415, (2005).
- ⁷ B. Balke, G. Fecher, J. Winterlik, and C. Felser, *Appl. Phys. Lett.* **90**, 152504 (2007).
- ⁸ H. Kurt, K. Rode, M. Venkatesan, P. Stamenov, and J. M. D. Coey, *Phys. Status Solidi B* **248**, 2338 (2011).
- ⁹ J. Winterlik, S. Chadov, A. Gupta, V. Alijani, T. Gasi, K. Filsinger, B. Balke, G. H. Fecher, C. A. Jenkins, F. Casper, J. Kübler, G. Liu, L. Gao, S. S. P. Parkin, and C. Felser, *Adv. Mater.* **24**, 6283 (2012).

¹⁰ I. Galanakis, in *Heusler Alloys*, Springer Series in Materials Science 222, C. Felser and A. Hirohata (eds.), Springer International Publishing Switzerland 2016.

¹¹ X. Wang, "Proposal for a New Class of Materials: Spin Gapless Semiconductors", *Phys. Rev. Lett.* **100**, 156404 (2008).

¹² P. Kharel, W. Zhang, R. Skomski, S. Valloppilly, Y. Huh, R. Fuglsby, S. Gilbert, and D. Sellmyer, "Magnetism and electron transport in a rapidly quenched CoFeCrAl nanomaterial" *J. Phys. D: Appl. Phys.* **48**, 245002 (2015).

¹³ S. Ouardi, G. H. Fecher, and C. Felser, "Realization of Spin Gapless Semiconductors: The Heusler Compound Mn₂CoAl", *Phys. Rev. Lett.* **110**, 100401 (2013).

¹⁴ R. Dhakal, S. Nepal, I. Galanakis, R.P. Adhikari, G.C. Kaphle, *J. Alloys Compd.*, **882**, 160500 (2021).

¹⁵ Q. Gao, I. Opahle, and H. Zhang, *Phys. Rev. Materials* **3**, 024410 (2019).

¹⁶ P. Lukashev, S. McFadden, P. Shand, P. Kharel, *J. Magn. Magn. Mater.* **584**, 171107 (2023).

¹⁷ E. O'Leary, B. Dahal, P. Kharel, and P. Lukashev, *J. Magn. Magn. Mater.* **514**, 167188 (2020).

¹⁸ G. Kresse and D. Joubert, *Phys. Rev. B* **59**, 1758 (1999).

¹⁹ P. Blöchl, *Phys. Rev. B* **50**, 17953 (1994).

²⁰ J. Perdew, K. Burke, and M. Ernzerhof, *Phys. Rev. Lett.* **77**, 3865 (1996).

²¹ M. Methfessel and A. T. Paxton, *Phys. Rev. B* **40**, 3616 (1989).

²² MedeA-2.22, Materials Design, Inc., San Diego, CA, USA, 2017.

²³ J. Towns, T. Cockerill, M. Dahan, I. Foster, K. Gaither, A. Grimshaw, V. Hazlewood, S. Lathrop, D. Lifka, G. D. Peterson, R. Roskies, J. R. Scott, N. Wilkins-Diehr, "XSEDE: Accelerating Scientific Discovery", *Computing in Science & Engineering*, vol.**16**, no. 5, pp. 62-74, Sept.-Oct. 2014.

²⁴ I. Tunic, J. Herran, B. Staten, P. Gray, T. Paudel, A. Sokolov, E. Tsymbal, and P. Lukashev; *J. Phys.: Condens. Matter* **29**, 075801 (2017).